15. Tateno C, Yoshizane Y, Saito N, Kataoka M, Utoh R, Yamasaki C, et al. Near completely humanized liver in mice shows human-type metabolic responses to drugs. Am J Pathol 2004;165:901-912.
16. Tsuge M, Hiraga N, Takaishi H, Noguchi C, Oga H, Imamura M, et al. Infection of human hepatocyte chimeric mouse with genetically engineered hepatitis B virus. HEPATOLOGY 2005;42:1046-1054.
17. Tsuge M, Hiraga N, Akiyama R, Tanaka S, Matsushita M, Mitsui F, et al. HBx protein is indispensable for development of viraemia in human hepatocyte chimeric mice. J Gen Virol 2010;91:1854-1864.
18. Kuhober A, Pudollek HP, Reifenberg K, Chisari FV, Schlicht HJ, Reimann J, Schirmbeck R. DNA immunization induces antibody and cytotoxic T cell responses to hepatitis B core antigen in H-2b mice. J Immunol 1996;156:3687-3695.
19. Banchereau J, Steinman RM. Dendritic cells and the control of immunity. Nature 1998;392:245-252.
20. Shortman K, Liu YJ. Mouse and human dendritic cell subtypes. Nat Rev Immunol 2002;2:151-161.
21. Sandhu J, Shpitz B, Gallinger S, Hozumi N. Human primary immune response in SCID mice engrafted with human peripheral blood lymphocytes. J Immunol 1994;152:3806-3813.
22. Gonzalez SF, Lukacs-Kornek V, Kuligowski MP, Pitcher LA, Degn SE, Kim YA, et al. Capture of influenza by medullary dendritic cells via SIGN-R1 is essential for humoral immunity in draining lymph nodes. Nat Immunol 2010;11:427-434.
23. Fernandez NC, Lozier A, Flament C, Ricciardi-Castagnoli P, Bellet D, Suter M, et al. Dendritic cells directly trigger NK cell functions: cross-talk relevant in innate anti-tumor immune responses *in vivo*. Nat Med 1999;5:405-411.
24. Ferlazzo G, Tsang ML, Moretta L, Melioli G, Steinman RM, Munz C. Human dendritic cells activate resting natural killer (NK) cells and are recognized via the NKp30 receptor by activated NK cells. J Exp Med 2002;195:343-351.
25. Andoniou CE, van Dommelen SL, Voigt V, Andrews DM, Brizard G, Asselin-Paturel C, et al. Interaction between conventional dendritic cells and natural killer cells is integral to the activation of effective antiviral immunity. Nat Immunol 2005;6:1011-1019.
26. Walzer T, Dalod M, Robbins SH, Zitvogel L, Vivier E. Natural-killer cells and dendritic cells: "l'union fait la force". Blood 2005;106:2252-2258.
27. Mosier DE, Gulizia RJ, Baird SM, Wilson DB, Spector DH, Spector SA. Human immunodeficiency virus infection of human-PBL-SCID mice. Science 1991;251:791-794.
28. Kawahara T, Douglas DN, Lewis J, Lund G, Addison W, Tyrrell DL, et al. Critical role of natural killer cells in the rejection of human hepatocytes after xenotransplantation into immunodeficient mice. Transpl Int 2010;23:934-943.
29. Morosan S, Hez-Deroubaix S, Lunel F, Renia L, Giannini C, Van Rooijen N, et al. Liver-stage development of *Plasmodium falciparum*, in a humanized mouse model. J Infect Dis 2006;193:996-1004.
30. Dorshkind K, Pollack SB, Bosma MJ, Phillips RA. Natural killer (NK) cells are present in mice with severe combined immunodeficiency (SCID). J Immunol 1985;134:3798-3801.
31. Ito M, Hiramatsu H, Kobayashi K, Suzue K, Kawahata M, Hioki K, et al. NOD/SCID/gamma(c)(null) mouse: an excellent recipient mouse model for engraftment of human cells. Blood 2002;100:3175-3182.
32. Thimme R, Wieland S, Steiger C, Ghrayeb J, Reimann KA, Purcell RH, Chisari FV. CD8(+) T cells mediate viral clearance and disease pathogenesis during acute hepatitis B virus infection. J Virol 2003;77:68-76.
33. Rehermann B, Fowler P, Sidney J, Person J, Redeker A, Brown M, et al. The cytotoxic T lymphocyte response to multiple hepatitis B virus polymerase epitopes during and after acute viral hepatitis. J Exp Med 1995;181:1047-1058.
34. Webster GJ, Reignat S, Maini MK, Whalley SA, Ogg GS, King A, et al. Incubation phase of acute hepatitis B in man: dynamic of cellular immune mechanisms. HEPATOLOGY 2000;32:1117-1124.
35. Zou Y, Chen T, Han M, Wang H, Yan W, Song G, et al. Increased killing of liver NK cells by Fas/Fas ligand and NKG2D/NKG2D ligand contributes to hepatocyte necrosis in virus-induced liver failure. J Immunol 2010;184:466-475.
36. Newman KC, Riley EM. Whatever turns you on: accessory-cell-dependent activation of NK cells by pathogens. Nat Rev Immunol 2007;7:279-291.
37. Galle PR, Hofmann WJ, Walczak H, Schaller H, Otto G, Stremmel W, et al. Involvement of the CD95 (APO-1/Fas) receptor and ligand in liver damage. J Exp Med 1995;182:1223-1230.
38. Rivero M, Crespo J, Fábrega E, Casafont F, Mayorga M, Gomez-Fleitas M, Pons-Romero F. Apoptosis mediated by the Fas system in the fulminant hepatitis by hepatitis B virus. J Viral Hepat 2002;9:107-113.
39. Moretta A. Natural killer cells and dendritic cells: rendezvous in abused tissues. Nat Rev Immunol 2002;2:957-964.
40. Asselin-Paturel C, Trinchieri G. Production of type I interferons: plasmacytoid dendritic cells and beyond. J Exp Med 2005;202:461-465.
41. Orito E, Ichida T, Sakugawa H, Sata M, Horiike N, Hino K, et al. Geographic distribution of hepatitis B virus (HBV) genotype in patients with chronic HBV infection in Japan. HEPATOLOGY 2001;34:590-594.

特集II　B型肝炎の抗ウイルス療法の進歩と耐性

# HBV RT領域変異株におけるテノホビルの抗ウイルス効果の検討*

柘植雅貴**
平賀伸彦**
茶山一彰**

**Key Words**：hepatitis B virus(HBV), human hepatocyte chimeric mouse, nucleotide analogue, drug resistant, tenofovir

## はじめに

2000年以降，B型慢性肝炎に対する治療薬としてラミブジン(ゼフィックス®，LMV)，アデフォビル(ヘプセラ，ADV)，エンテカビル(バラクルード®，ETV)といった核酸アナログ製剤が保険適応となり，B型慢性肝炎治療の中心的薬剤となっている．核酸アナログ製剤は，B型肝炎ウイルス(HBV)の増殖過程において，ウイルスポリメラーゼに取り込まれ，chain terminatorとしてマイナス鎖合成時の逆転写反応やプラス鎖合成時の伸長反応を阻害することで，強力な抗ウイルス効果を発揮する．しかしながら，強力な抗ウイルス効果の反面，核酸アナログ治療による感染肝細胞からHBV完全排除はきわめて困難であり，多くの症例で，数年に及ぶ核酸アナログ治療が行われているのが現状である．その結果，一部の症例では，HBVポリメラーゼ遺伝子RT領域のアミノ酸変異が生じ，薬剤耐性を獲得したHBVが増殖することによってviral breakthroughやbreakthrough hepatitisを発症しており，薬剤耐性HBVに対する治療法の確立が大きな課題となっている[1)~4)]．

当研究室では，*in vitro*および*in vivo*におけるHBV複製・感染モデルを確立し，ポリメラーゼ領域の変異に伴うHBVに対する各種核酸アナログ製剤の抗ウイルス効果を評価し，報告してきた[2)3)5)]．本稿では，その*in vitro*および*in vivo*の薬効評価系を用いて，ポリメラーゼ領域の変異株に対するテノホビル(TDF)の抗ウイルス効果を評価したので報告する．

## *In vitro* HBV複製系を用いた薬効評価系の構築

B型慢性肝炎症例に対して核酸アナログ製剤を長期間使用すると，HBVポリメラーゼ遺伝子のRT領域で生じたアミノ酸変異に伴い，HBVは薬剤耐性を獲得する．特にRT領域にあるYMDD motif(RT領域203～206番アミノ酸)のメチオニン(M)がバリン(V)やイソロイシン(I)へと変異すると，高度なLMV耐性を獲得する[6)7)]．そこで，さまざまな薬剤耐性変異について解析するため，HBV感染患者の血清からHBVゲノムを抽出し，1.4倍長のHBVゲノムをベクターに挿入したHBV発現プラスミド(野生株)を作製した．さらに，これらのプラスミドのRT領域にHBVの薬剤耐性変異を加え，薬剤耐性HBV発現プラスミドを作製した．作製したHBVクローンは，図1に示すように，野生株に加え，LMV耐性変異であるrtL180M/rtM204V変異を加えたrtL180M/rtM204V株，LMV/ADV耐性

* Anti-viral effects of tenofovir for HBV mutants.

** Masataka TSUGE, M.D., Ph.D., Nobuhiko HIRAGA, M.D., Ph.D. & Kazuaki CHAYAMA, M.D., Ph.D.: 広島大学病院消化器・代謝内科〔〒734-8551 広島県広島市南区霞1-2-3〕; Department of Medicine and Molecular Science, Graduate School of Biomedical Sciences, Hiroshima University, Hiroshima 734-8551, JAPAN

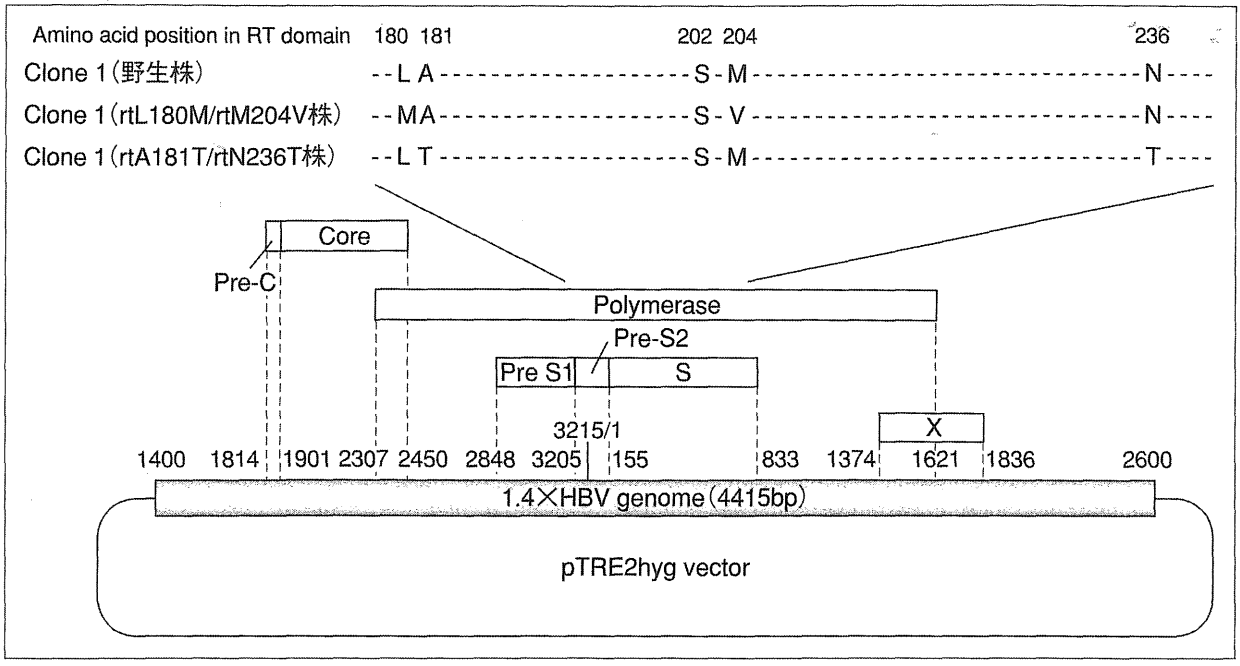


図1　本検討に使用したHBV発現プラスミドの構造と薬剤耐性変異導入部位

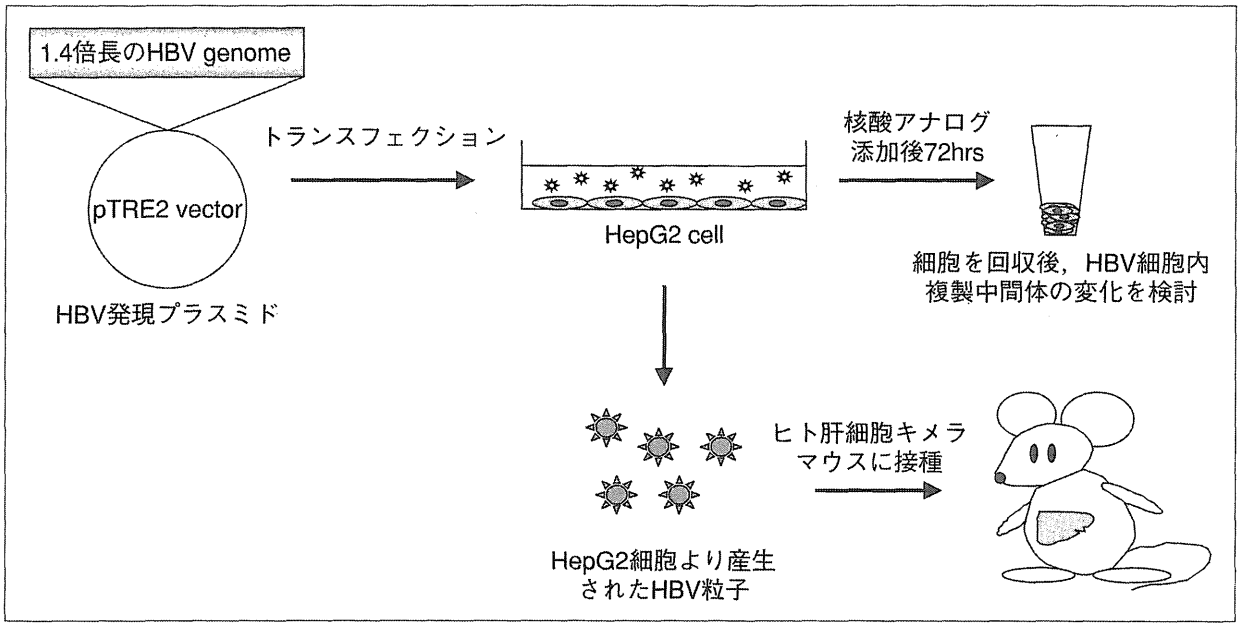


図2　本研究の流れ

HBV感染患者血清をもとに作製したHBV発現プラスミドをHepG2細胞にトランスフェクション．24時間後より，培養上清中に核酸アナログを添加し，72時間後に細胞を回収．細胞内のHBV複製中間体を定量し，抗ウイルス効果を検討（*in vitro*）．また，HBV発現プラスミドをトランスフェクションしたHepG2細胞から産生されたHBV粒子を回収し，ヒト肝細胞キメラマウスの尾静脈より接種．HBV感染が成立後，マウスに核酸アナログを経口投与し，マウス血清中のHBV DNAの変化を解析し，核酸アナログの抗ウイルス効果を検討（*in vivo*）．

rtA181T/rtN236T変異を加えたrtA181T/rtN236T株の3種類である．これらのプラスミドをHepG2細胞にトランスフェクションし，その後，培養上清中に核酸アナログを添加．72時間後に細胞を回収し，細胞内複製中間体量を測定することによって，*in vitro*でのHBVクローンの核酸アナログの感受性を評価した（図2）．

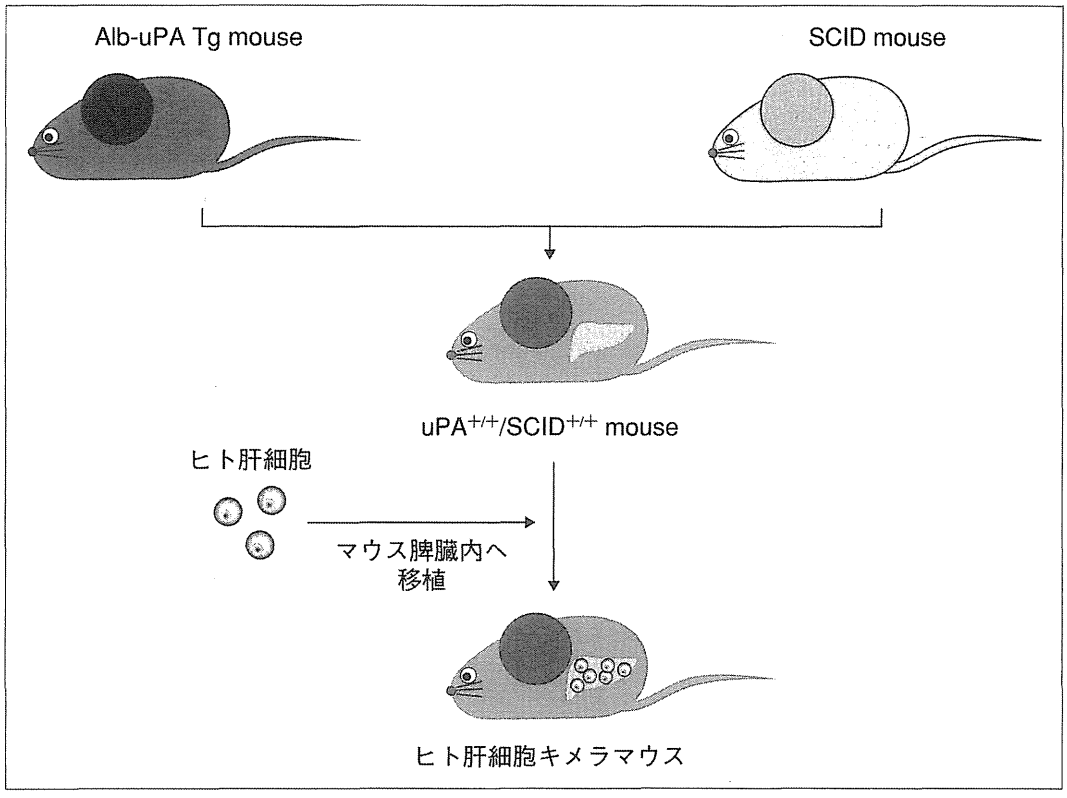


図3　ヒト肝細胞キメラマウスの構築
Alb-uPAトランスジェニックマウスとSCIDマウスを交配させ，uPA$^{+/+}$/SCID$^{+/+}$マウスを作製．同マウスに対し，経脾的にヒト肝細胞を移植．ヒト肝細胞は，マウス肝臓内で生着し，ヒト肝細胞キメラマウスが作製される．（文献[10]より引用改変）

## *In vivo* HBV感染・複製モデルを用いた薬効評価系の構築

HBVは，マウスやラットといった小動物には感染せず，ヒトやチンパンジーといった特定の動物のみに感染する．そのため，*in vivo*におけるHBV研究は，チンパンジーを用いて行われてきたが，チンパンジーはワシントン条約で保護されていること，飼育費用は高額で，飼育施設の確保も困難であることから，十分な研究ができなかった．近年，ヒト肝細胞をマウスに移植することによって，マウス肝臓が高度にヒト肝細胞へと置換されたヒト肝細胞キメラマウスが開発され[8][9]，本学でも，吉里らの研究により，uPA-SCIDマウスを用いたヒト肝細胞キメラマウスの作製が可能となった[10]．uPA-SCIDマウスは，アルブミン(Alb)プロモーター下にurokinase-type plasminogen activator(uPA)を遺伝子導入したAlb-uPA Tgマウスと重症免疫不全を呈するsevere combined immune deficient(SCID)マウスを交配させ，作製されたマウスであり，生後uPAが肝細胞内で高発現することによりマウスの肝細胞は壊死に陥り，肝不全を呈する．このuPA-SCIDマウスに，ヒト肝細胞を経脾的に移植することにより，マウス肝臓が高度にヒト肝細胞に置換されたヒト肝細胞キメラマウスが作製される(図3)．

本マウスの尾静脈よりHBV感染患者血清を接種すると，接種後2週目よりマウス血清中のHBV DNAは検出可能となり，その後徐々に上昇し，8～10log copies/ml程度に達し，24週間以上感染は持続する(図4)．このHBV持続感染マウスにLMVを経口投与すると，マウス血清中のHBV DNAは速やかに低下することから，HBVが持続感染したヒト肝細胞キメラマウスを用いて薬効評価が可能であることが示された[5]．

## 野生株に対するTDFの抗ウイルス効果の検討

はじめに，各種核酸アナログの抗ウイルス効果を比較するため，HBV野生株であるClone 1(野

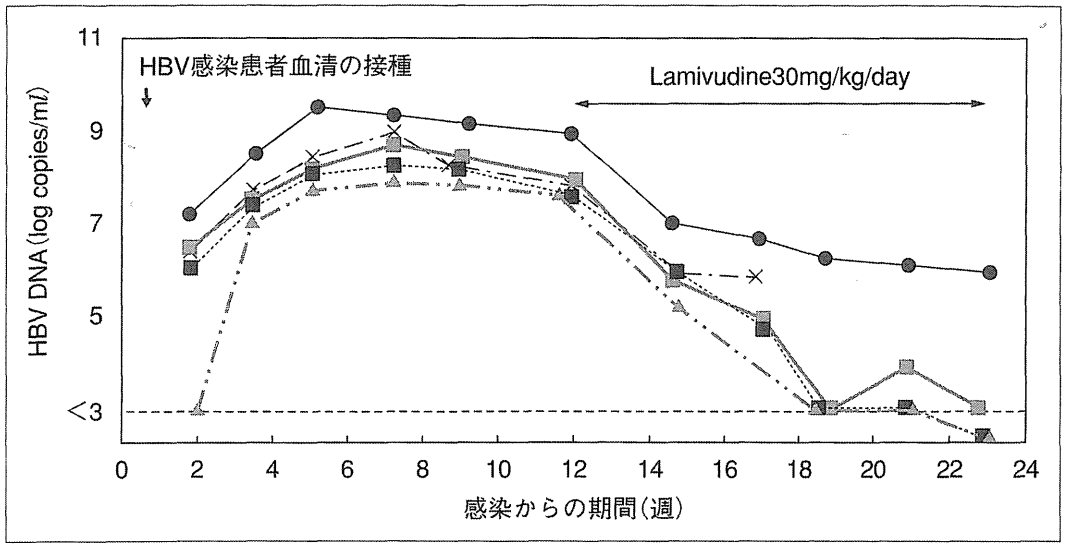


図4　HBV持続感染キメラマウスの作製とLMVによる抗ウイルス効果
ヒト肝細胞キメラマウスにHBV感染患者血清を接種．マウス血清中のHBV DNAは徐々に上昇し，8～10log copies/mlに達した．このマウスに対し，感染12週目よりLMVを経口投与したところ，マウス血清HBV DNAは減少し，LMVの抗ウイルス効果が確認された．（文献[5]より引用改変）

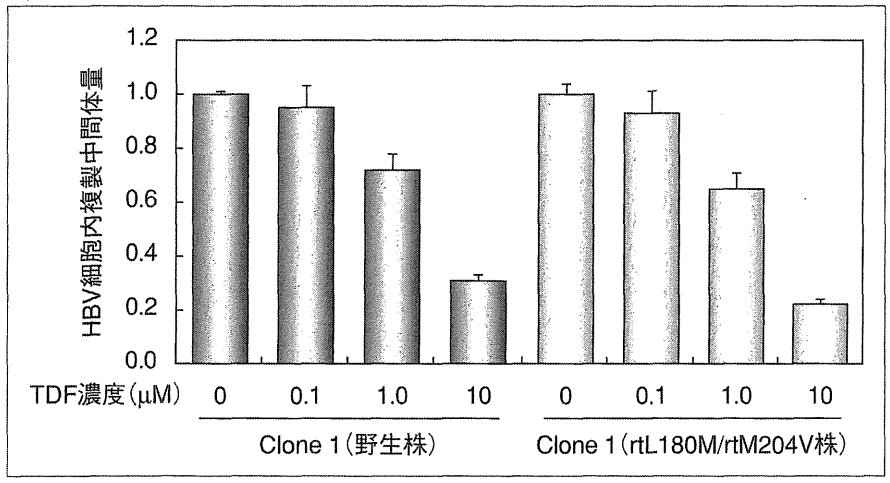


図5　*In vitro*におけるTDFの抗ウイルス効果の検討(野生株 vs. LMV耐性株)
*In vitro*のHBV複製モデルを用いて，TDF濃度の変化に伴うHBV細胞内複製中間体量の変化について検討．いずれのクローンにおいても複製中間体はTDFの濃度依存的に低下し，その低下の程度は，野生株，LMV耐性株いずれにおいてもほぼ同程度であった．

生株)を用いて，*in vitro*での検討を行った．野生株のHBV発現プラスミドをHepG2細胞にトランスフェクションし，24時間後より培養上清中に核酸アナログを添加し，添加72時間後の細胞内の複製中間体量の変化をreal time PCR法を用いて検討した．その結果，図5に示すように，TDFの濃度依存的にHBV細胞内複製中間体量は減少することが確認された．そこで，*in vitro*における結果を確認するため，培養上清より産生させたHBV粒子(野生株)をヒト肝細胞キメラマウスに接種し，*in vivo*での抗ウイルス効果についても検討した．使用した3頭いずれにおいても，マウス血中のHBV DNA量はTDF投与により速やかに低下し，4週間で平均3.6logの低下を認めた．その他3種類の核酸アナログ製剤を使用した場合と比較すると，LMV投与では4週間で3.0log，ADVでは1.7log，ETVでは4.2logの低下であったことから，TDFの抗ウイルス効果はほぼ同等であるものと考えられた(図6)．これらの結果から，TDFは核酸アナログ初回投与例において，

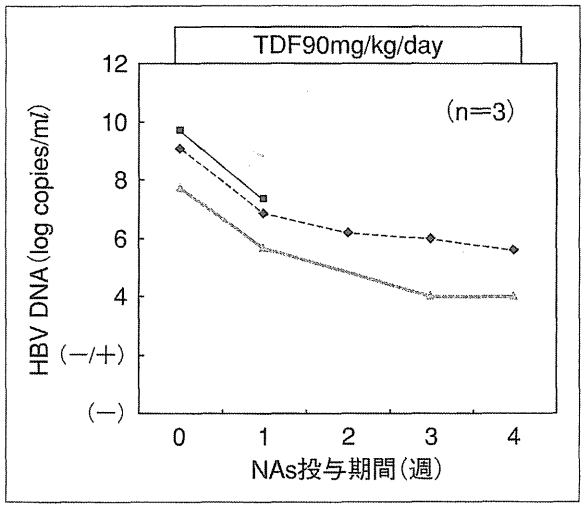


図6 *In vivo*における野生株に対するTDFの抗ウイルス効果の検討
野生株の感染したヒト肝細胞キメラマウスに対してTDF投与し，マウス血清HBV DNAの変化を検討．HBV DNAはTDF投与により，速やかに低下し，4週間で平均3.6log copies/m*l*の低下を認めた．

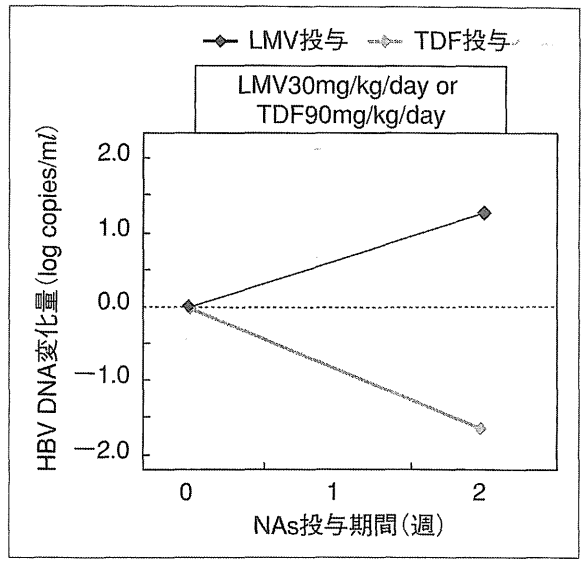


図7 *In vivo*におけるLMV耐性株に対するTDFの抗ウイルス効果の検討
LMV耐性変異をもつrtL180M/rtM204V株を感染させたヒト肝細胞キメラマウスに対してTDF投与し，マウス血清HBV DNAの変化を検討．HBV DNAはTDF投与により，2週間で1.6log copies/m*l*の低下を認めた．

臨床的にも有効である可能性が示された．

## LMV耐性株に対するTDFの抗ウイルス効果の検討

B型慢性肝炎症例に対し，LMV長期投与を行うと，投与1年で約20%，2年で30～40%の患者に耐性ウイルスが出現し，これらの耐性ウイルス出現に伴うbreak through hepatitisを起こすことが知られている．本検討では，このLMV耐性変異として頻度が高いrtL180M/rtM204V株を作製し，*in vitro*および*in vivo*の検討を行った．rtL180M/rtM204V株のプラスミドをHepG2細胞にトランスフェクションし，TDFによる抗ウイルス効果を検討したところ，野生株と同様，TDFの濃度依存的な抗ウイルス効果が確認された．そこで，野生株とのTDF感受性を比較すると，各濃度におけるHBV細胞内複製中間体の変化率はほぼ同程度であり，LMV耐性株に対して，野生株とほぼ同等の抗ウイルス効果が期待できるものと考えられた(図5)．そこで，野生株同様，*in vitro*において作製したLMV耐性HBV粒子をヒト肝細胞キメラマウスの尾静脈より接種し，LMV耐性HBV持続感染マウスを作製し，LMVおよびTDFの経口投与を行った．その結果，2週間のTDF投与により，マウス血中のHBV DNA量は1.6logの低下を認めたが，LMV投与ではまったくHBV DNAの低下は認められなかった(図7)．

## LMV/ADV耐性株を用いた抗ウイルス効果の検討

現在，B型慢性肝炎患者において，前述の如く，LMV耐性を認めた症例に対してはLMVとADVの併用療法が行われている．本邦では，ADVはLMV耐性症例に対する対応策として開発されたことから，現在もLMV耐性例に対してLMVとの併用療法が行われていることが多い．同治療法は，ADV単独投与に比べ，耐性獲得の頻度が低いとされているものの，長期投与例では，LMV単独投与例と同様に，LMV, ADVのいずれにも耐性を示す多剤耐性変異株が出現することがわかってきた[11)12)]．そこで，LMV/ADV両剤耐性株として知られるrtA181T/rtN236T株を作製し，同様の検討を行った．LMV/ADV耐性株をトランスフェクションしたHepG2細胞に対し，TDFを添加したところ，TDFの濃度依存的にHBV細胞内複製中間体の減少が確認でき，その減少率は野生株とほぼ同程度であった(図8)．そこで，同ウイルスクローンを用いて同様の検討を*in vivo*において施行した．その結果，TDF投与にて2週間で3.0logの低下を認め，野生株と比較

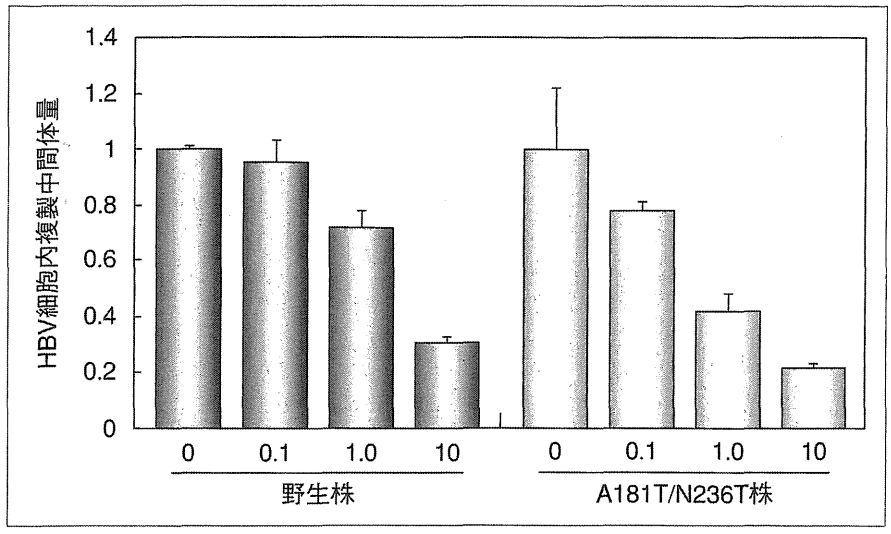


図8　*In vitro*におけるTDFの抗ウイルス効果の検討(野生株 vs. LMV/ADV耐性株)
*In vitro* HBV複製モデルを用いて，TDFによる野生株およびLMV/ADV耐性株への抗ウイルス効果について検討．いずれのクローンにおいても複製中間体はTDFの濃度依存的に低下し，その低下の程度は，ほぼ同程度であった．

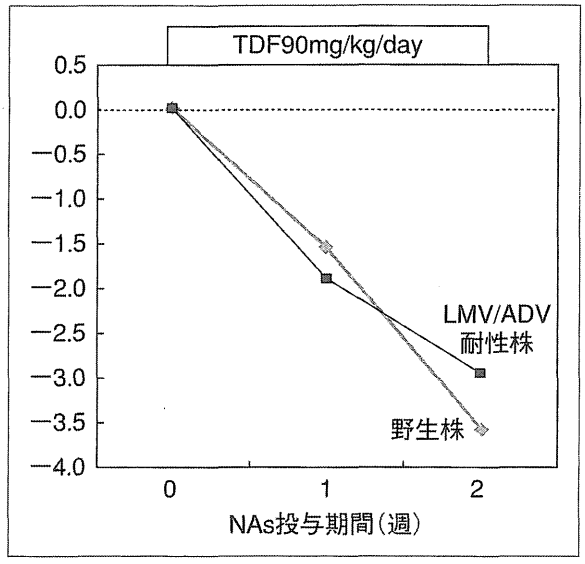


図9　*In vivo*における野生株とLMV/ADV耐性株(A181T/N236T株)のTDF感受性の比較
野生株およびLMV/ADV耐性株の感染したヒト肝細胞キメラマウスに対してTDF投与．マウス血清HBV DNAの変化を検討したところ，いずれのHBVクローンにおいても速やかなHBV DNAの低下が確認され，その低下量も野生株で−3.6log, LMV/ADV耐性株で−3.0logと同等の低下が認められた．

してもほぼ同程度の感受性であることが示された(図9)．

## 今後の展望

現在，B型慢性肝炎に対する新たな治療薬として，TDFの治験が進行中である．TDFは，海外での使用報告からみると，HBVに対する抗ウイルス効果は非常に強力であり，また耐性株の出現率も低いと考えられる．2000年以降，B型慢性肝炎治療において核酸アナログ製剤は欠かせない治療薬となってきており，各種核酸アナログ製剤を用いることによって，多剤耐性を獲得したHBVの増加が懸念されている．本研究では，野生株に加え，LMV耐性株，LMV/ADV耐性株に対するTDFの抗ウイルス効果について検討を行った．しかしながら，本研究に用いた耐性ウイルスは，これまで報告されている耐性ウイルスのごく一部にすぎず，その他の耐性変異についてもTDFが良好な抗ウイルス効果を示すか否かを検討していく必要がある．今後，TDFが臨床で使用可能となることが予測されることから，TDFに対して耐性を示す変異株についても検討を追加し，核酸アナログを用いた新たな治療戦略を構築していくことが重要であると考えられた．

## 文　献

1) Lok AS, Zoulim F, Locarnini S, et al. Antiviral drug-resistant HBV : standardization of nomenclature and assays and recommendations for management. Hepatology 2007 ; 46 : 254.

2) Yatsuji H, Hiraga N, Mori N, et al. Successful treatment of an entecavir-resistant hepatitis B virus variant. J Med Virol 2007 ; 79 : 1811.
3) Yatsuji H, Noguchi C, Hiraga N, et al. Emergence of a novel lamivudine-resistant hepatitis B virus variant with a substitution outside the YMDD motif. Antimicrob Agents Chemother 2006 ; 50 : 3867.
4) Zoulim F, Locarnini S. Hepatitis B virus resistance to nucleos(t)ide analogues. Gastroenterology 2009 ; 137 : 1593.
5) Tsuge M, Hiraga N, Takaishi H, et al. Infection of human hepatocyte chimeric mouse with genetically engineered hepatitis B virus. Hepatology 2005 ; 42 : 1046.
6) Allen MI, Deslauriers M, Andrews CW, et al. Identification and characterization of mutations in hepatitis B virus resistant to lamivudine. Lamivudine Clinical Investigation Group. Hepatology 1998 ; 27 : 1670.
7) Tipples GA, Ma MM, Fischer KP, et al. Mutation in HBV RNA-dependent DNA polymerase confers resistance to lamivudine in vivo. Hepatology 1996 ; 24 : 714.
8) Brown JJ, Parashar B, Moshage H, et al. A long-term hepatitis B viremia model generated by transplanting nontumorigenic immortalized human hepatocytes in Rag-2-deficient mice. Hepatology 2000 ; 31 : 173.
9) Mercer DF, Schiller DE, Elliott JF, et al. Hepatitis C virus replication in mice with chimeric human livers. Nat Med 2001 ; 7 : 927.
10) Tateno C, Yoshizane Y, Saito N, et al. Near completely humanized liver in mice shows human-type metabolic responses to drugs. Am J Pathol 2004 ; 165 : 901.
11) Perrillo R, Hann HW, Mutimer D, et al. Adefovir dipivoxil added to ongoing lamivudine in chronic hepatitis B with YMDD mutant hepatitis B virus. Gastroenterology 2004 ; 126 : 81.
12) Yatsuji H, Suzuki F, Sezaki H, et al. Low risk of adefovir resistance in lamivudine-resistant chronic hepatitis B patients treated with adefovir plus lamivudine combination therapy : two-year follow-up. J Hepatol 2008 ; 48 : 923.

* * *

Digestive Diseases

Dig Dis 2012;30:580–587
DOI: 10.1159/000343070

# Usefulness of the Multimodality Fusion Imaging for the Diagnosis and Treatment of Hepatocellular Carcinoma

Yuki Makino[a] Yasuharu Imai[a] Takumi Igura[a] Hideko Ohama[a] Sachiyo Kogita[a]
Yoshiyuki Sawai[a] Kazuto Fukuda[a] Hiroshi Ohashi[b] Takamichi Murakami[c]

Departments of [a]Gastroenterology and [b]Pathology, Ikeda Municipal Hospital, Ikeda, and [c]Department of Radiology, Kinki University School of Medicine, Osaka-Sayama, Japan

**Key Words**
US fusion imaging · CT fusion imaging · Fusion imaging · Volume Navigation System · Hepatocellular carcinoma · Radiofrequency ablation · Gd-EOB-DTPA · Sonazoid

**Abstract**
A multimodality fusion imaging system has been introduced for the clinical practice of diagnosis and treatment of hepatocellular carcinoma (HCC), especially for loco-regional treatment. An ultrasonography (US) fusion imaging system can provide a side-by-side display of real-time US images and any cross-sectional images of multiplanar reconstruction of CT or MRI that synchronize real-time US. The US fusion imaging system enables us to perform radiofrequency ablation (RFA) for HCCs difficult to detect on conventional US safely. Besides, we can evaluate the treatment effects of RFA easily at the bedside by combining the contrast-enhanced US and the US fusion imaging system. Fusion images of pre- and post-RFA CT have been utilized for the assessment of the treatment effects of RFA. Although the treatment effects of RFA have been conventionally evaluated, comparing pre- and post-RFA CT side-by-side, the evaluation tends to be inaccurate. On CT fusion images, the tumor and the ablation zone are overlaid and we can grasp the positional relation easily, leading to quantitative and more accurate evaluation. The multimodality fusion imaging system has become quite an important tool for loco-regional treatment of HCC because of its usefulness for both the guidance during the RFA procedure and the evaluation of its treatment effects.



## Introduction

Recently, imaging technology in CT, MRI and ultrasonography (US) for the diagnosis of hepatocellular carcinoma (HCC) has dramatically progressed. In addition, contrast media such as Sonazoid (Daiichi-Sankyo, Tokyo, Japan), one of the second-generation US contrast agents, and gadolinium-ethoxybenzyl-diethylenetriamine pentaacetic acid (Gd-EOB-DTPA) (Primovist; Bayer HealthCare, Osaka, Japan), a liver-specific contrast MR agent have become available [1–9]. As a result, the diagnosis of HCC has come to be made at an earlier stage. However, it is occasionally difficult to perform needle-based loco-re-

KARGER
Fax +41 61 306 12 34
E-Mail karger@karger.ch
www.karger.com


0257–2753/12/0306–0580$38.00/0

Accessible online at:
www.karger.com/ddi

Yasuharu Imai, MD, PhD
Department of Gastroenterology
Ikeda Municipal Hospital
3-1-18, Johnan, Ikeda, Osaka 563-8510 (Japan)
E-Mail yasuimai@hosp.ikeda.osaka.jp

gional treatment such as radiofrequency ablation (RFA) and percutaneous ethanol injection therapy for early HCCs, since some of them are not clearly visualized on grayscale US [10].

Along with the progress in diagnostic imaging, a multimodality fusion imaging system has been developed for the clinical practice of treatment of HCC, particularly for the assistance of loco-regional treatment. It has been reported that HCCs hardly detectable on conventional grayscale US could be detected with subsequent loco-regional treatment by virtue of the US fusion imaging system [1, 10–15]. In addition to the US fusion imaging system, a CT fusion imaging system has been reported to be useful for accurate assessment of treatment effects of RFA [16–19]. This report aims to review the usefulness of the multimodality fusion imaging system for percutaneous loco-regional treatment of HCC.

## Outline of the US Fusion Imaging System

The US fusion imaging system, such as the Volume Navigation System (GE Healthcare Japan, Tokyo, Japan) [1, 15] and Real-time Virtual Sonography (Hitachi Medico, Co., Tokyo, Japan) [11–14] enables the synchronized display of real-time US images and multiplanar reconstruction (MPR) images of CT or MRI corresponding to the cross section of real-time US. The MPR images are reconstructed based on the volume data of CT or MR images and displayed as a reference, side-by-side, with real-time US images on a single screen.

The US fusion imaging system is useful for the accurate diagnosis and treatment of HCC with safety, in particular at the time of percutaneous loco-regional procedures. It has been reported that the US fusion imaging system is helpful in the detection of HCCs which are difficult to recognize on grayscale US [1, 14, 15]. Therefore, even if the diagnosis of HCC is made at an early stage and the tumor is not detected on US, percutaneous loco-regional treatments can be conducted using the US fusion imaging system. Besides the guidance of loco-regional treatments, the US fusion imaging system can be applied to the evaluation of treatment effects of RFA [13].

The Volume Navigation System, one of the multimodality fusion imaging systems commercially available since 2009 in Japan, is equipped with an ultrasound unit LOGIQ E9 (GE Healthcare Japan) (fig. 1). In Volume Navigation System, the following steps are needed for the synchronized display of real-time US images and CT or MR images.

First, the volume data of CT or MR images for reference should be imported into the system in the digital imaging and communication in medicine (DICOM) format, through a network or a recording media such as CD-ROM or USB-HDD. After the volume data is imported, US images are displayed on the left side of the screen and CT or MR images on the right side, as a reference. In order to synchronize real-time US images to the reference, the cross section of US images approximately parallel to the axial image of the reference has to be registered. Next, two magnetic positioning sensors attached to the probe of an ultrasound scanner (a in fig. 1) detect the magnetic field radiated from a magnetic field transmitter (b in fig. 1) and transmit the information of spatial location and orientation of the probe to a magnetic position-detecting unit (c in fig. 1) equipped with LOGIQ E9. In this way, a magnetic position-detecting unit integrates the positional information of two magnetic positioning sensors and reconstructs MPR images which match the 3D information of the sensors. Subsequently, real-time US and reference images are synchronously displayed in accordance with the movement of the probe. However, since these two image sets are not exactly matched at this time yet, further positional registration of real-time US and reference images is needed. A common point on US and reference images should be visualized for the registration. Practically, we have to visualize a characteristic landmark on US images and mark the point. After marking the landmark point, the US image is fixed and we should operate the probe to seek the corresponding landmark on reference images, by comparing it with the fixed US image. When the landmark point on the reference image is marked, the registration is completed. Then, US and reference images are matched and simultaneously displayed, side by side, on the same screen.

In addition to the simultaneous display of real-time US images and a reference, the Volume Navigation System is equipped with the global positioning system (GPS) function. After positional registration, when GPS markers are indicated on the target on reference images, corresponding sites are pinpointed on real-time US images. This GPS function provides several advantages: firstly, since the site where the target should be visible is pinpointed on real-time US images, it is helpful to detect the target on US, even if it is difficult to perceive on conventional US, and secondly, once the GPS markers are indicated on a target, the target can easily be detected by anyone and from any scanning section, by referring to the GPS markers. Thirdly, it can be applied to the evaluation of treatment effects of RFA, as described later.

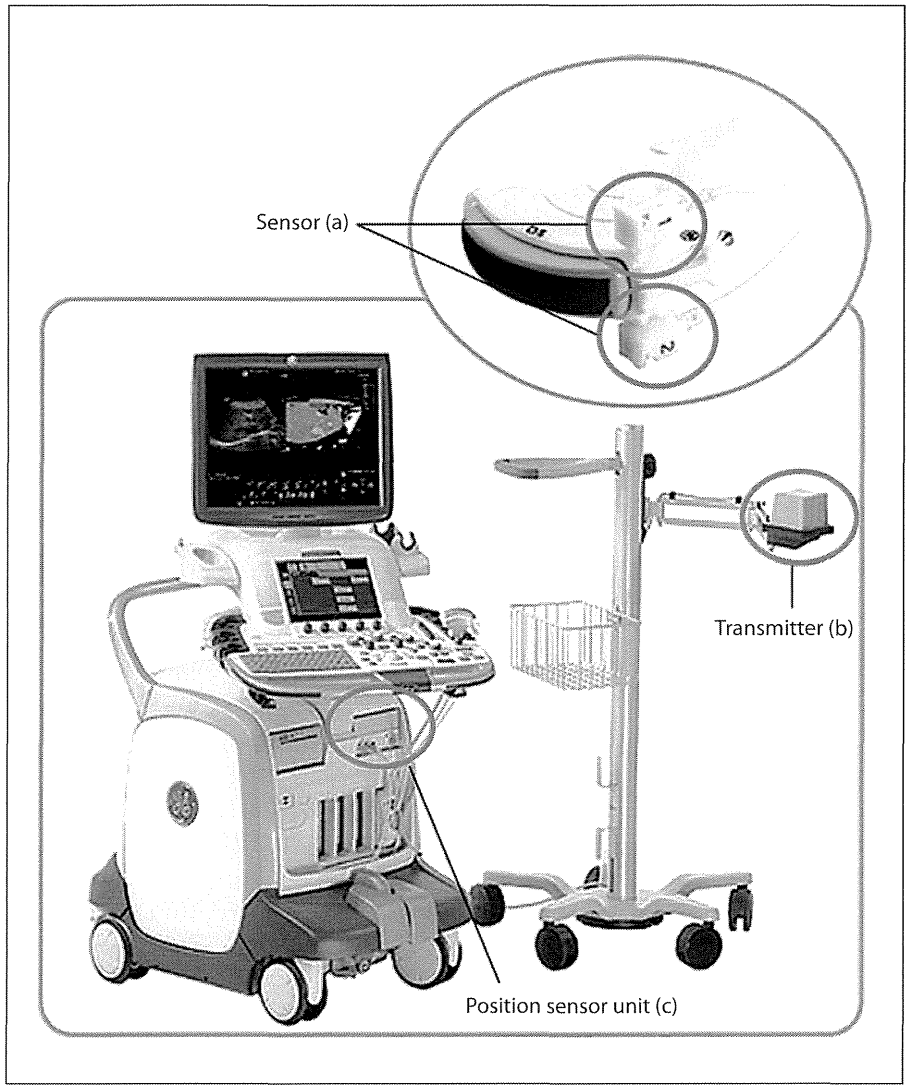


**Fig. 1.** An outline of the Volume Navigation System. Two magnetic positioning sensors (a), a magnetic field transmitter (b), and a position sensor unit installed in the body of an ultrasound system (c) are needed for the Volume Navigation System. A magnetic field transmitter can be set anywhere at the bedside. Two magnetic positioning sensors are attached to the US probe and the positional information of each sensor is compared in order to evaluate the accuracy of it. The positional information of magnetic positioning sensors is sent to a magnetic position-detecting unit and MPR images which synchronize real-time US images are reconstructed based on this.

### Application of the US Fusion Imaging System to the Guidance of Percutaneous Loco-Regional Treatments

Since Gd-EOB-DTPA-enhanced MRI has been clinically available, the diagnosis of HCC tends to be made at an earlier stage than before [1–5]. Accordingly, HCCs difficult to recognize on grayscale US have become detectable as hypointense nodules on hepatobiliary phase of Gd-EOB-DTPA-enhanced MRI. The US fusion imaging system effectively serves as assistance in the diagnosis and percutaneous loco-regional treatment of such HCCs.

Figure 2 shows a case of HCC in which needle core tumor biopsy and RFA using US fusion imaging system were carried out. Although the hypovascular nodule in segment III was depicted as a hypointense nodule on the hepatobiliary phase of Gd-EOB-DTPA-enhanced MRI, it was undetectable either on dynamic CT, grayscale US, or Sonazoid-enhanced US (fig. 2a–c). With the Volume Navigation System using the hepatobiliary phase of Gd-EOB-DTPA-enhanced MRI as a reference, we performed US-guided target biopsy of the site corresponding to the nodule on reference images, using intrahepatic vessels and hepatic contours as landmarks (fig. 2c). The pathological diagnosis was well-differentiated HCC (fig. 2d). After the diagnosis of HCC, we conducted RFA

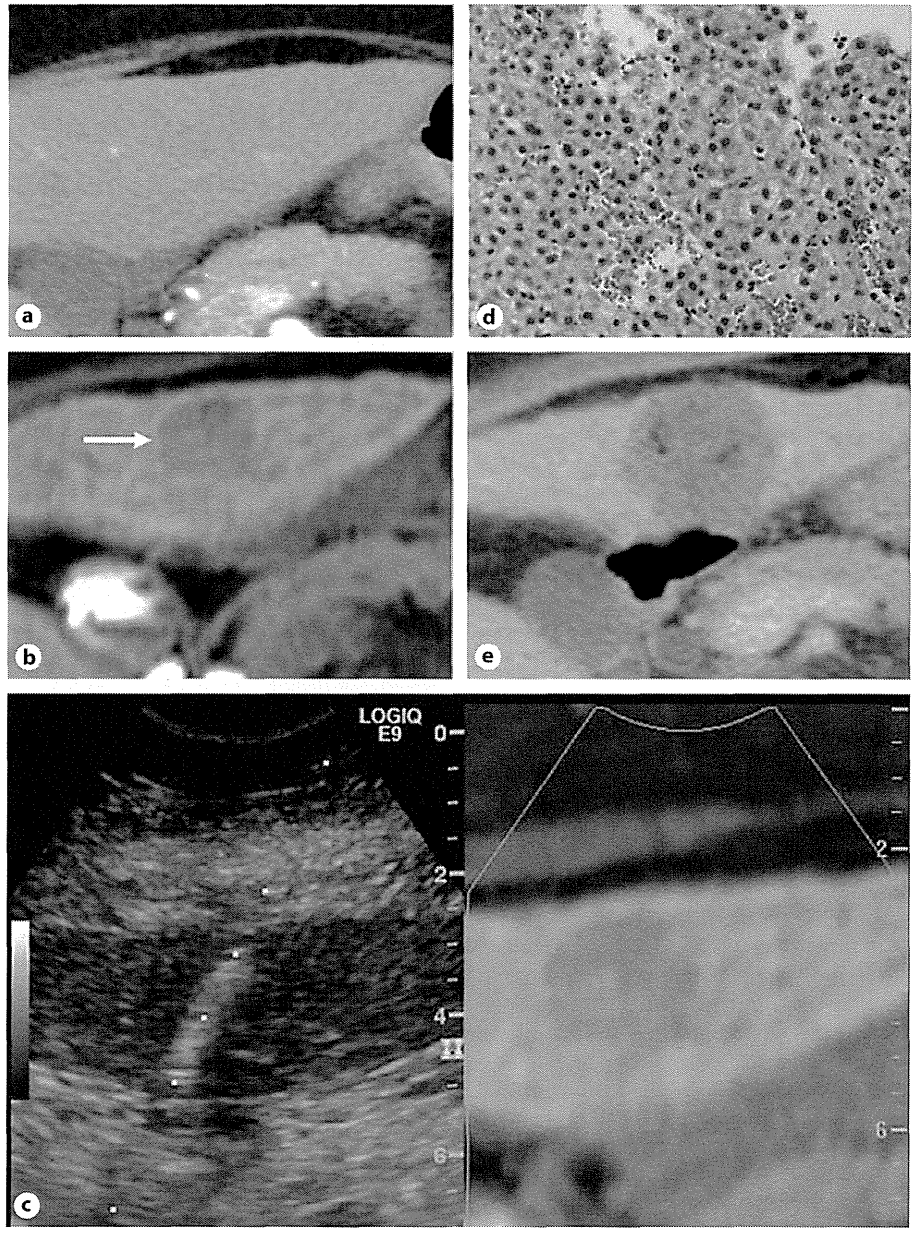


**Fig. 2.** Needle core biopsy and RFA with guidance from an US fusion imaging system in an 80-year-old woman with hypovascular HCC. **a** Arterial phase of pre-RFA dynamic CT. **b** Hepatobiliary phase of Gd-EOB-DTPA-enhanced MRI. **c** Fusion images of pre-RFA grayscale US and hepatobiliary phase of Gd-EOB-DTPA-enhanced MRI using the Volume Navigation System. **d** Histology of the biopsy specimen of the nodule in segment III (HE staining). **e** Portal phase of post-RFA dynamic CT. The nodule in segment III was detected on neither grayscale US, Sonazoid-enhanced US, or dynamic CT. Only the hepatobiliary phase of Gd-EOB-DTPA-enhanced MRI could identify the hypointense nodule 27 mm in diameter (arrow), which was suspected of being a hypovascular HCC. Therefore, using the hepatobiliary phase of Gd-EOB-DTPA-enhanced MRI as a reference, needle core biopsy was performed with the Volume Navigation System and the nodule was proven to be a well-differentiated HCC. Subsequently, RFA was carried out with the Volume Navigation System in the same way, and the tumor was completely ablated.

in the same way with the guidance of the Volume Navigation System. The dynamic CT at 3 days after RFA revealed complete ablation of the tumor (fig. 2e). In this way, percutaneous target biopsy or loco-regional treatment can be performed with the assistance of US fusion imaging system, even if the nodule is undetectable either on conventional grayscale US or contrast-enhanced US.

The utility of the US fusion imaging system has also been reported in several studies [10–15]. Kunishi et al. [15] reported that US fusion imaging combining conventional US and the hepatobiliary phase of Gd-EOB-DTPA-enhanced MRI was more sensitive than conventional US or contrast-enhanced US for the detection of HCCs, especially small or atypical HCCs, which was quite similar to our results.

Thus, the indication of percutaneous loco-regional treatment seems to have been greatly extended by virtue of the US fusion imaging system.

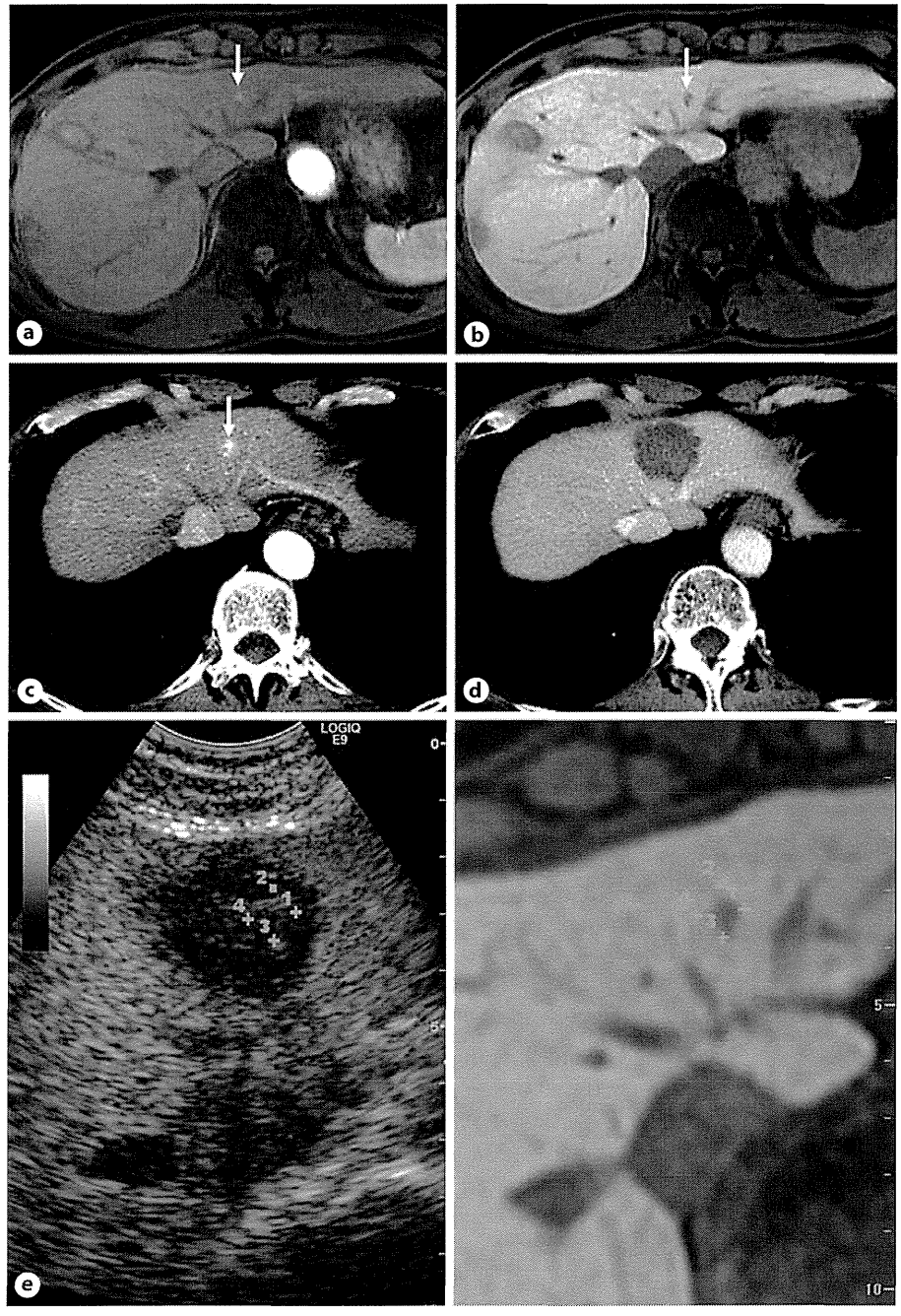


**Fig. 3.** US fusion imaging system for the evaluation of treatment effects of RFA in a 57-year-old man with hypervascular HCC. **a** Arterial phase of pre-RFA Gd-EOB-DTPA-enhanced MRI. **b** Hepatobiliary phase of pre-RFA Gd-EOB-DTPA-enhanced MRI. **c** Arterial phase of pre-RFA dynamic CT. **d** Portal phase of post-RFA dynamic CT. **e** Fusion images of post vascular phase of contrast-enhanced US (left side) and hepatobiliary phase of Gd-EOB-DTPA-enhanced MRI (right side). The tumor was visualized as an early enhancing nodule on both the arterial phase of Gd-EOB-DTPA-enhanced MRI and dynamic CT, and as a hypointense nodule on the hepatobiliary phase of Gd-EOB-DTPA-enhanced MRI in segment III (arrow). Following RFA, contrast-enhanced US using Sonazoid was performed at the bedside to evaluate the treatment effects with the Volume Navigation System using the GPS function. The hepatobiliary phase of Gd-EOB-DTPA-enhanced MRI was used as reference. After marking four points on the margin of the tumor on the reference image (**e**; right side), the corresponding four points were displayed on real-time US (**e**; left side). In the post-vascular phase of Sonazoid-enhanced US, these four points were fully encompassed within the hypoechoic area of the ablation zone, indicating complete ablation. Complete ablation was also confirmed on dynamic CT after RFA.

### Application of the US Fusion Imaging System in the Evaluation of the Treatment Effects of RFA

The US fusion imaging system is useful not only for the guidance of loco-regional treatment, but also for the assessment of the treatment effects of RFA [13]. Since an ablated tumor becomes obscure on US during RFA due to surrounding high echoic bubbles, it is difficult to evaluate the treatment effects of RFA using conventional US. However, by using the GPS function of the US fusion imaging system described above, the treatment effects can be easily evaluated at the bedside by comparing the ablated area depicted as a low echoic area on the post-vascular phase of Sonazoid-enhanced US with the

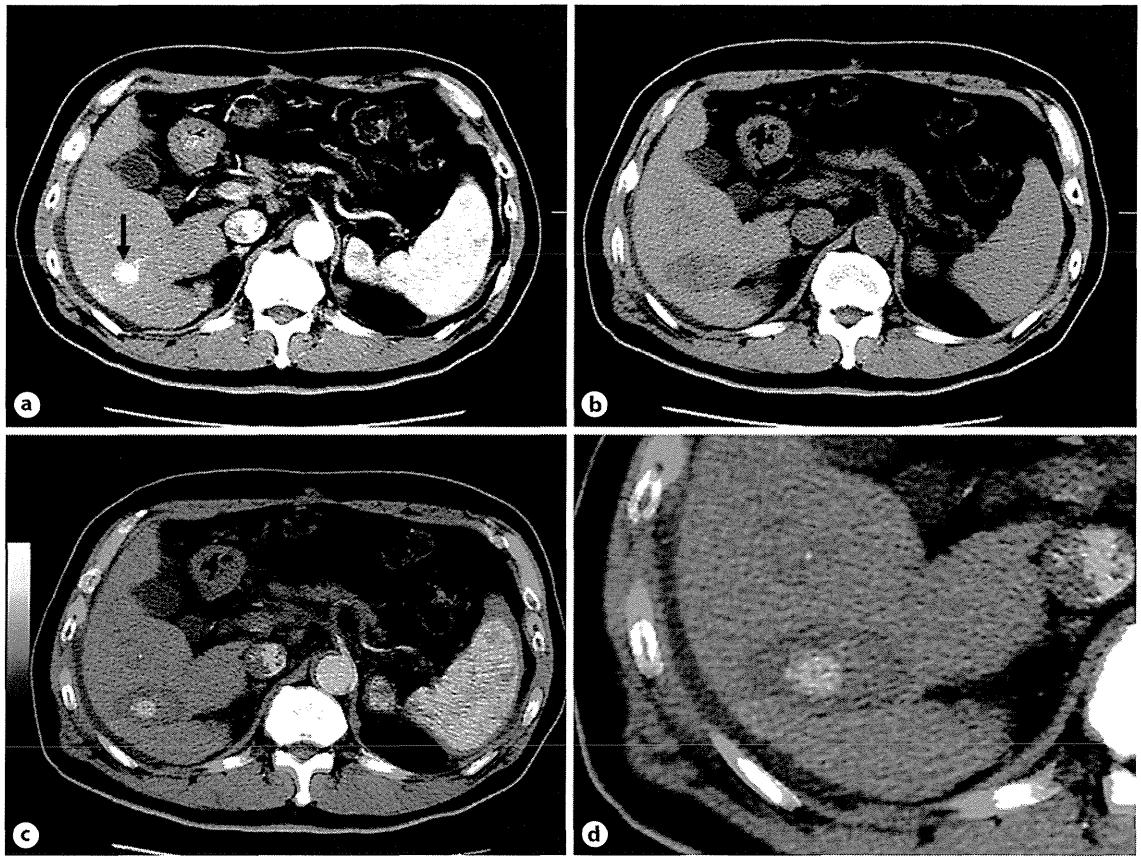

**Fig. 4.** CT fusion imaging system for the evaluation of treatment effects of RFA in a 68-year-old man with hypervascular HCC. **a** Arterial phase of pre-RFA dynamic CT. **b** Portal phase of post-RFA dynamic CT. **c** Fusion image of pre- and post-RFA CT. **d** Fusion image of pre- and post-RFA CT (enlarged). The hypervascular HCC in segment VI (arrow) was treated with RFA. Compared with side-by-side interpretation of pre- and post-RFA CT, the positional relationship becomes clear and it becomes possible to evaluate the ablative margin accurately on CT fusion images.

tumor on the reference images. One example is demonstrated in figure 3. The tumor on hepatobiliary phase of Gd-EOB-DTPA-enhanced MRI, used as a reference, was considered to be covered by the low echoic area on the post-vascular phase of Sonazoid-enhanced US performed after RFA, which becomes quite comprehensive using the GPS function. Since the volume data of US, as well as those of CT and MRI, can also be used as a reference, US images of pre- and post-RFA can be compared.

Although inherent limitations still remain in terms of the accuracy, due to difficulty in the fusion technology of volume data of US, the US fusion imaging system is useful for the assessment of the treatment effects of RFA by virtue of its convenience, minimal invasiveness, and real-time characteristics.

## CT Fusion Imaging System for the Evaluation of Treatment Effects of RFA

For the evaluation of treatment effects of RFA using dynamic CT, pre- and post-RFA CT have been conventionally compared in a side-by-side manner. However, since it is quite difficult to comprehend the locational relationship of the tumor and ablation zone graphically in this side-by-side interpretation, the assessment tends to be subjective and inaccurate.

Recently, to overcome these problems, fusion images of pre- and post-RFA CT have been utilized for judging the curative effects of RFA [16–19]. Figure 4 shows the case of an HCC patient who underwent RFA and the treatment effects were assessed using a CT fusion imaging system. CT fusion images are created with Advantage

Workstation VolumeShare 4 (GE Healthcare Japan). After automatic alignment of pre- and post-RFA CT using the rigid registration method, manual registration was added by referencing to intrahepatic structures such as blood vessels, cysts, or the iodized oil from previous treatments, and hepatic contours around the tumor. Since pretreatment tumor and the ablation zone are overlaid, it becomes easy to grasp the positional relation of the tumor and the ablation zone visually, resulting in more accurate evaluation of the treatment effects of RFA.

At Ikeda Municipal Hospital, a CT fusion imaging system was introduced for the evaluation of treatment effects of RFA in 2011. Now, the creation of CT fusion images of RFA are performed as routine daily work by radiological technicians, and these images can be seen on patients' charts for use in deciding whether to administer additional RFA. The application of a CT fusion imaging system to the evaluation of treatment effects of RFA is just getting started, and it is hoped to be widely used hereafter.

## Conclusion

The present state of the multimodality fusion imaging system and its usefulness in the diagnosis and treatment of HCC were outlined in this review. Since US fusion imaging systems have been introduced into clinical practice, it has become possible to perform percutaneous loco-regional treatment for tumors which are difficult to detect on conventional US, but detectable on other imaging modalities, particularly on the hepatobiliary phase of Gd-EOB-DTPA-enhanced MRI. As another multimodality fusion imaging system, CT fusion imaging technology provides more accurate evaluation of the treatment effects of RFA than the conventional side-by-side assessment.

Imaging diagnosis of HCC has been progressing remarkably in recent years. The important thing is to make the best use of the advanced imaging modalities, combining the strong points of each modality complementarily. In particular, multimodality fusion imaging seems to play an important role in the diagnosis and treatment of HCC.

## Disclosure Statement

The authors declare that no financial or other conflict of interest exists in relation to the content of the article.

## References

1 Murakami T, Imai Y, Okada M, Hyodo T, Lee WJ, Kim MJ, Kim T, Choi BI: Ultrasonography, computed tomography and magnetic resonance imaging of hepatocellular carcinoma: toward improved treatment decisions. Oncology 2011;81:86–99.
2 Kudo M: Diagnostic imaging of hepatocellular carcinoma: recent progress. Oncology 2011;81(suppl 1):73–85.
3 Kogita S, Imai Y, Okada M, Kim T, Onishi H, Takamura M, Fukuda K, Igura T, Sawai Y, Morimoto O, Hori M, Nagano H, Wakasa K, Hayashi N, Murakami T: Gd-EOB-DTPA-enhanced magnetic resonance images of hepatocellular carcinoma: correlation with histological grading and portal blood flow. Eur Radiol 2010;20:2405–2413.
4 Onishi H, Kim T, Imai Y, Hori M, Nagano H, Nakaya Y, Tsuboyama T, Nakamoto A, Tatsumi M, Kumano S, Okada M, Takamura M, Wakasa K, Tomiyama N, Murakami T: Hypervascular Hepatocellular carcinomas: detection with gadoxetate disodium-enhanced MR imaging and multiphasic multidetector CT. Eur Radiol 2012;22:845–854.
5 Sano K, Ichikawa T, Motosugi U, Sou H, Muhi AM, Matsuda M, Nakano M, Sakamoto M, Nakazawa T, Asakawa M, Fujii H, Kitamura T, Enomoto N, Araki T: Imaging study of early hepatocellular carcinoma: usefulness of gadoxetic acid-enhanced MR imaging. Radiology 2011;261:834–844.
6 Kudo M, Hatanaka K, Kumada T, Toyoda H, Tada T: Double-contrast ultrasound: a novel surveillance tool for hepatocellular carcinoma. Am J Gastroenterol 2011;106:368–370.
7 Moriyasu F, Itoh K: Efficacy of perflubutane microbubble-enhanced ultrasound in the characterization and detection of focal liver lesions: phase 3 multicenter clinical trial. AJR Am J Roentgenol 2009;193:86–95.
8 Lee JM, Yoon JH, Joo I, Woo HS: Recent advances in CT and MR imaging for evaluation of hepatocellular carcinoma. Liver Cancer 2012;1:22–40.
9 Ricke J, Seidensticker M, Mohnike K: Noninvasive diagnosis of hepatocellular carcinoma in cirrhotic liver: current guidelines and future prospects for radiological imaging. Liver Cancer 2012;1:51–58.
10 Kim YJ, Lee MW, Park HS: Small hepatocellular carcinomas: ultrasonography guided percutaneous radiofrequency ablation. Abdom Imaging 2012, E-pub ahead of print.
11 Minami Y, Chung H, Kudo M, Kitai S, Takahashi S, Inoue T, Ueshima K, Shiozaki H: Radiofrequency ablation of hepatocellular carcinoma: value of virtual CT sonography with magnetic navigation. AJR Am J Roentgenol 2008;190:335–341.
12 Nakai M, Sato M, Sahara S, Takasaka I, Kawai N, Minamiguchi H, Tanihata H, Kimura M, Takeuchi N: Radiofrequency ablation assisted by real-time virtual sonography and CT for hepatocellular carcinoma undetectable by conventional sonography. Cardiovasc Intervent Radiol 2009;32:62–69.
13 Minami Y, Kitai S, Kudo M: Treatment response assessment of radiofrequency ablation for hepatocellular carcinoma: usefulness of virtual CT sonography with magnetic navigation. Eur J Radiol 2012;81:e277–e220.

14 Liu FY, Yu XL, Liang P, Cheng ZG, Han ZY, Dong BW, Zhang XH, Rennert J, Georgieva M, Schreyer AG, Jung W, Ross C, Stroszczynski C, Jung EM: Microwave ablation assisted by a real-time virtual navigation system for hepatocellular carcinoma undetectable by conventional ultrasonography. Eur J Radiol 2012;81:1455–1459.
15 Kunishi Y, Numata K, Morimoto M, Okada M, Kaneko T, Maeda S, Tanaka K: Efficacy of fusion imaging combining sonography and hepatobiliary phase MRI with Gd-EOB-DTPA to detect small hepatocellular carcinoma. AJR Am J Roentgenol 2012;198:106–114.
16 Fujioka C, Horiguchi J, Ishifuro M, Kakizawa H, Kiguchi M, Matsuura N, Hieda M, Tachikake T, Alam F, Furukawa T, Ito K: A feasibility study: evaluation of radiofrequency ablation therapy to hepatocellular carcinoma using image registration of preoperative and postoperative CT. Acad Radiol 2006; 13:986–994.
17 Giesel FL, Mehndiratta A, Locklin J, McAuliffe MJ, White S, Choyke PL, Knopp MV, Wood BJ, Haberkorn U, von Tengg-Kobligk H: Image fusion using CT, MRI and PET for treatment planning, navigation and follow up in percutaneous RFA. Exp Oncol 2009;31: 106–114.
18 Kim YS, Lee WJ, Rhim H, Lim HK, Choi D, Lee JY: The minimal ablative margin of radiofrequency ablation of hepatocellular carcinoma (>2 and <5 cm) needed to prevent local tumor progression: 3D quantitative assessment using CT image fusion. AJR Am J Roentgenol 2010;195:758–765.
19 Kim KW, Lee JM, Klotz E, Kim SJ, Kim SH, Kim JY, Han JK, Choi BI: Safety margin assessment after radiofrequency ablation of the liver using registration of preprocedure and postprocedure CT images. AJR Am J Roentgenol 2011;196:565–572.